Systematic and Applied Microbiology 46 (2023) 126404

Contents lists available at ScienceDirect

Systematic and Applied Microbiology

journal homepage: www.elsevier.com/locate/syapm

# Dominance of mixed ether/ester, intact polar membrane lipids in five species of the order *Rubrobacterales*: Another group of bacteria not obeying the "lipid divide"

Jaap S. Sinninghe Damsté [a,b,*], W. Irene C. Rijpstra [a], Katharina J. Huber [c], Luciana Albuquerque [d], Conceição Egas [d,e], Nicole J. Bale [a]

[a] NIOZ Royal Netherlands Institute for Sea Research, Department of Marine Microbiology and Biogeochemistry, Texel, the Netherlands
[b] Department of Earth Sciences, Faculty of Geosciences, Utrecht University, Utrecht, the Netherlands
[c] Department of Microorganisms, Leibniz-Institute DSMZ – Deutsche Sammlung von Mikroorganismen und Zellkulturen, D-38124 Braunschweig, Germany
[d] CNC - Center for Neuroscience and Cell Biology, UC-Biotech, Biocant Park, 3060-197, Cantanhede, Portugal
[e] BIOCANT – Transfer Technology Association, Biocant Park, 3060-197 Cantanhede, Portugal

ARTICLE INFO

*Keywords:*
*Rubrobacterales*
1-O-alkyl glycerol ether lipids
Intact polar lipids
ω-cyclohexyl fatty acids
(ω-4)-methyl fatty acids
*Rubrobacter radiotolerans*
*R. xylanophilus*
*R. bracarensis*
*R. calidifluminis*
*R. naiadicus*

ABSTRACT

The composition of the core lipids and intact polar lipids (IPLs) of five *Rubrobacter* species was examined. Methylated (ω-4) fatty acids (FAs) characterized the core lipids of *Rubrobacter radiotolerans*, *R. xylanophilus* and *R. bracarensis*. In contrast, *R. calidifluminis* and *R. naiadicus* lacked ω-4 methyl FAs but instead contained abundant (i.e., 34–41 % of the core lipids) ω-cyclohexyl FAs not reported before in the order *Rubrobacterales*. Their genomes contained an almost complete operon encoding proteins enabling production of cyclohexane carboxylic acid CoA thioester, which acts as a building block for ω-cyclohexyl FAs in other bacteria. Hence, the most plausible explanation for the biosynthesis of these cyclic FAs in *R. calidifluminis* and *R. naiadicus* is a recent acquisition of this operon. All strains contained 1-O-alkyl glycerol ether lipids in abundance (up to 46 % of the core lipids), in line with the dominance (>90 %) of mixed ether/ester IPLs with a variety of polar headgroups. The IPL head group distribution of *R. calidifluminis* and *R. naiadicus* differed, e.g. they lacked a novel IPL tentatively assigned as phosphothreoninol. The genomes of all five *Rubrobacter* species contained a putative operon encoding the synthesis of the 1-O-alkyl glycerol phosphate, the presumed building block of mixed ether/ester IPLs, which shows some resemblance with an operon enabling ether lipid production in various other aerobic bacteria but requires more study. The uncommon dominance of mixed ether/ester IPLs in *Rubrobacter* species exemplifies our recent growing awareness that the lipid divide between archaea and bacteria/eukaryotes is not as clear cut as previously thought.

## Introduction

The species of the genus *Rubrobacter* represent one of the deepest phylogenetic branches of the phylum *Actinomycetota* (Salam et al., 2020; Oren and Garrity, 2021) (formerly called 'Actinobacteria' or the high G + C gram-positive bacteria). The first two isolated strains of the genus *Rubrobacter* were extremophilic microorganisms. The type species of the genus, *Rubrobacter radiotolerans*, was isolated from a gamma-irradiated hot spring (Yoshinaka et al., 1973; Suzuki et al., 1988) and was found to be extremely resistant to gamma radiation (Suzuki et al., 1988; Ferreira et al., 1999). The species *R. xylanophilus* was isolated from the hot run-off of a factory and had an optimal

*Abbreviations:* 1-MGE, mono glycerol *sn*-1 ether; AEG, acyl/ether glycerol; CHC-CoA, cyclohexane carboxylic acid CoA thioester; DAG, diacylglycerol; DMDS, dimethyl disulfide; DMPE, dimethyl phosphoethanolamine; DPG, diphosphatidylglycerol; ECL, equivalent chain length; FA, fatty acid; GC, gas chromatography; Hex-PHex, hexose-phosphohexose; HexA-Hex, hexosamine-hexose; IPL, intact polar lipid; MGE, mono glycerol ether; MS, mass spectrometry; PC, phosphocholine; PG, phosphoglycerol; PG-Hex, phosphoglycerol-hexose; PSI-BLAST, position-specific iterated BLAST; PT, phosphothreoninol; SQ, sulfoquinovosyl; TLC, thin-layer chromatography; UHPLC-HRMS, ultra-high-pressure liquid chromatography–high resolution mass spectrometry.

* Corresponding author at: NIOZ Royal Netherlands Institute for Sea Research, Department of Marine Microbiology and Biogeochemistry, PO Box 59, 1790 AB Den Burg, the Netherlands.

*E-mail address:* jaap.damste@nioz.nl (J.S. Sinninghe Damsté).

https://doi.org/10.1016/j.syapm.2023.126404
Received 12 December 2022; Revised 26 January 2023; Accepted 20 February 2023

growth temperature of 60 °C and, hence, is thermophilic (Carreto et al., 1996), and also resistant to gamma radiation (Ferreira et al., 1999). Currently, nine other species have been isolated and taxonomically validly described (i.e., *R. taiwanensis* (Chen et al., 2004); *R. bracarensis* (Jurado et al., 2012); *R. calidifluminis* and *R. naiadicus* (Albuquerque et al., 2014); *R. aplysinae* (Kämpfer et al., 2014); *R. spartanus* (Norman et al., 2017); *R. indicoceani* (Chen et al., 2018), and *R. marinus* and *R. tropicus* (Chen et al., 2020). Interestingly, not all these *Rubrobacter* species are thermophiles, some of these were isolated from biofilms of the wall of a church (*R. bracarensis*) or marine environments, such as deep-sea sediments (*R. indicoceani, R. marinus* and *R. tropicus*) or a sponge (*R. aplysinae*). Relatives of *Rubrobacter* spp. occur widely in the natural environment with a high diversity, e.g., in marine sediments (Chen et al., 2021) and in desert soils, where they are estimated to form 3–10 % of the microbial population (Holmes et al., 2000).

An intriguing aspect of the physiology of *Rubrobacter* spp. is their uncommon and specific lipid distribution. Members of the unusual series of ω-4 methyl fatty acids, i.e., 12-methyl hexadecanoic acid and 14-methyl octadecanoic acid, often occur in relatively high abundance (Suzuki et al., 1988; Carreto et al., 1996). In the thermophilic species, *R. xylanophilus* and *R. taiwanensis,* 14-methyl octadecanoic acid is the most abundant fatty acid (Albuquerque et al., 2014), whilst in the mesophilic species, i.e., *R. aplysinae, R. indicoceani*, *R. marinus* and *R. tropicus*, 12-methyl hexadecanoic acid is the prominent fatty acid (Albuquerque et al., 2014; Norman et al., 2017). In moderately thermophilic strains, i.e., *R. bracarensis* and *R. spartanus* (Albuquerque et al., 2014; Norman et al., 2017), both ω-4 methyl fatty acids occur. Remarkably, despite their close phylogenetic relationship to the other *Rubrobacter* spp., the thermophilic species *R. calidifluminis* and *R. naiadicus* do not contain ω-4 methyl fatty acids (Albuquerque et al., 2014). However, they produce in abundance (20–30 % of total fatty acids) a $C_{20}$ fatty acid with an unknown structure, in addition to $C_{17}$ and $C_{18}$ iso fatty acids and some other unknowns. The intact polar lipids (IPLs) of *Rubrobacter* spp. have so far not been studied with modern mass spectrometric (MS) methods; they have typically been characterized with two-dimensional thin-layer chromatography (TLC), which only led to the tentative identification of some general IPL classes.

Here we (re)investigate the lipid composition of five different *Rubrobacter* species, including *R. calidifluminis* and *R. naiadicus* for which the main fatty acids remain to be identified. In addition to conventional fatty acid analysis, we also identified other core lipids and studied intact polar lipids (IPLs) with ultra-high-pressure liquid chromatography–high resolution mass spectrometry (UHPLC-HRMS).

## Materials and methods

### *Cultivation*

All cultures were grown at DSMZ in 0.5 or 1 l Erlenmeyer flasks and were harvested in the transit of the late exponential phase to the beginning stationary phase. The strains *Rubrobacter calidifluminis* RG-1 $^{T}$ and *Rubrobacter naiadicus* RG-3 $^{T}$ were grown in DSMZ medium 1033 at 60 °C for three days, while *Rubrobacter bracarensis* DSM 24908 $^{T}$ was grown in the DSMZ medium 545, supplemented with 3 % NaCl (w/v; final concentration) and 2 % $MgSO_4$ (w/v; final concentration), at 28 °C for five days. The DSMZ medium 878, supplemented with 1 % NaCl (w/v; final concentration), was employed for cultivation of *Rubrobacter xylanophilus* DSM 9941 $^{T}$. The strain was incubated at 60 °C for ten days. The strain *Rubrobacter radiotolerans* DSM 5868 $^{T}$ was grown in the DSMZ medium 535 at 37 °C for five days. Details on the composition of the DSMZ media can be found on the DSMZ web page (https://www.dsmz.de/microorganisms/medium/).

The cells of all strains were harvested by centrifugation in either the Sorvall RC 6plus centrifuge (rotor F109-6x500y) at 9000 rpm for 20 min or in the Beckman coulter centrifuge Avanti® J-30I (rotor JA-14; Galway, IRE) at 10000 rpm for 20 min. After the liquid was removed the harvested cells were lyophilized overnight in a freeze-drying machine Christ Alpha 1–4 LDplus (Osterode am Harz, GER) at −60 °C and 0.025 mbar.

### *Lipid analysis*

Core lipid analysis was carried out at NIOZ by acid hydrolysis of total cell material with 5 % HCl in methanol by refluxing for 3 h, then derivatized by methylation of the acid groups with diazomethane. A first aliquot of this methylated extract was then silylated with pyridine (10 µl) and N,O-bis(trimethylsilyl)trifluoroacetamide (BSTFA, 10 µl), and analyzed by gas chromatography and gas chromatography–mass spectrometry (GC–MS), following procedures described previously (Sinninghe Damsté et al., 2011). For the identification of unknown fatty acids in *R. bracarensis* and *R. calidifluminis* the remaining methylated extract was eluted over an $Al_2O_3$ column with dichloromethane as the eluent, yielding an apolar fraction which was analyzed by GC–MS. Aliquots of the apolar fractions were subsequently subjected to hydrogenation with $PtO_2$ in ethyl acetate and reanalyzed by GC–MS. In case of *R. bracarensis* another aliquot of the apolar fraction was used to determine double bond positions of methylated fatty acids by dimethyl disulfide (DMDS) derivatization (Nichols et al., 1986).

Intact polar lipids (IPLs) were extracted from freeze-dried biomass using a modified Bligh–Dyer procedure (Bale et al., 2019) and analyzed by reverse phase UHPLC-HRMS$^{n}$ (Bale et al., 2021). An Agilent 1290 Infinity I UHPLC, equipped with thermostatted auto-injector and column oven, coupled to a Q Exactive Orbitrap mass spectrometer with an Ion Max source with a heated electrospray ionization probe (Thermo Fisher Scientific) was used. IPLs were separated on an Acquity BEH C18 column (Waters, 2.1 × 150 mm, 1.7 µm), maintained at 30 °C, using a flow rate of 0.2 mL $min^{-1}$. For this separation a mixture of two different eluents was used; eluent A was composed of a mixture of methanol and $H_2O$ (85:15, v:v) and eluent B of methanol and isopropanol (50:50, v:v). Both eluents were modified by addition of small amounts of formic acid (0.12 %, v/v) and 14.8 M $NH_3$aq (0.04 %, v/v). The elution program was as follows: 95 % A for 3 min, followed by a linear gradient to 40 % A at 12 min and then to 0 % A at 50 min. These latter conditions were maintained until 80 min. The settings for the electrospray ionization probe, operated in positive ion mode, were: capillary temperature, 300 °C; sheath gas ($N_2$) pressure, 40 arbitrary units (AU); auxiliary gas ($N_2$) pressure, 10 AU; spray voltage, 4.5 kV; probe heater temperature, 50 °C; S-lens 70 V. The Q Exactive mass spectrometer was calibrated within a mass accuracy range of 1 ppm using the Thermo Scientific Pierce LTQ Velos ESI Positive Ion Calibration Solution. The IPLs were analyzed with a mass range of *m/z* 350–2000 with a resolving power of 70,000 ppm at *m/z* 200. Data-dependent tandem MS/MS (resolving power 17,500 ppm) was successively performed by fragmentation of the 10 most abundant ions (stepped normalized collision energy 15, 22.5, 30; isolation width, 1.0 *m/z*). Dynamic exclusion was used to temporarily (for 6 s) exclude masses to allow selection of less abundant ions for MS/MS. Note that IPLs have varying degrees of ionization efficiency. Hence, the peak areas (in response units) of different IPLs do not necessarily reflect their actual relative abundance. However, this method allows for comparison between samples when analyzed in the same batch.

### *Extraction of DNA*

Total genomic DNA of strains *Rubrobacter calidifluminis* RG-1 $^{T}$ and *Rubrobacter naiadicus* RG-3 $^{T}$ was extracted following the method of Nielsen *et al.* (Nielsen et al., 1995). Cells were lysed with a solution

of lysozyme, guanidium thiocyanate and sodium *n*-lauryl sarcosine. DNA was extracted with chloroform:isoamyl alcohol (24:1, v/v), precipitated with isopropanol and washed with 70 % ethanol, dried and resuspended in water. RNase was included in the extraction process. The purity of DNA was verified by 1 % agarose gel electrophoresis. DNA quantity was measured by fluorescence in an Invitrogen Qubit 2.0 fluorometer (Thermo Fisher Scientific).

### *Genome sequencing, annotation and analysis*

The extracted DNA of *R. calidifluminis* RG-1 $^{T}$ and *R. naiadicus* RG-3 $^{T}$ was prepared for genome sequencing using the Nextera XT DNA Library Preparation Kit (Illumina) according to standard protocols. Bacterial genomes were sequenced on an MiSeq (Illumina) with PE 2x300 bp reads. Sequenced reads were filtered for quality with Trimmomatic version 0.39 (Bolger et al., 2014) and assembled with SPAdes version 3.14.1 (Bankevich et al., 2012). Genes were predicted with Prodigal version 2.6 (Hyatt et al., 2010), and annotated with Prokka version 1.14.6 (Seemann, 2014). rRNA and tRNA genes were detected with Barrnap version 0.9 (https://github.com/tseemann/barrnap). Genome estimated completeness and contamination were verified with CheckM version 1.2.0 (Parks et al., 2015). This Whole Genome Shotgun project has been deposited at DDBJ/ENA/GenBank under the accessions JAQKGV000000000 (*R. calidifluminis* RG-1 $^{T}$) and JAQKGW000000000 (*R. naiadicus* RG-3 $^{T}$). The versions described in this paper are version JAQKGV01000000 and JAQKGW01000000, respectively.

The genomes of R. radiotolerans DSM 5868 $^{T}$, *R. bracarensis* VF70612_S1$^{T}$, and *R. xylanophilus* PRD-1 $^{T}$ were obtained from the NCBI database. Genes involved in the lipid biosynthetic pathways were identified in the genomes of the *Rubrobacter* spp. using PSI-BLAST (Position-Specific iterated BLAST) searches at the protein level (https://www.ncbi.com) typically using two iteration steps using well defined proteins as query sequences using cut-off values of 1E-20 and 30 % identity.

## Results and discussion

Five different *Rubrobacter* species (Table 1) were analyzed for their IPL composition. To aid in their identification, acid hydrolysis of the Bligh-Dyer extracts was performed to identify the core lipids of these IPLs. The acid hydrolysis-released (core) lipids included both ester-bound fatty acids and ether-bound alkyl chains (detected as mono glycerol *sn*-1 ethers, 1-MGEs). Most fatty acid distributions have been reported previously but the major fatty acids of the species *R. calidifluminis* and *R. naiadicus* remained unknown (Albuquerque et al., 2014).

### *Core lipids*

The fatty acid distributions of *R. radiotolerans*, *R. xylanophilus* and *R. bracarensis* (Table 2) are quite similar and in agreement with those reported earlier for these species (Albuquerque et al., 2014) with 12-methyl hexadecanoic acid or its homologue, 14-methyl octadecanoic, as the most abundant fatty acids, comprising 35–50 % of the total sum of lipids. The unknown fatty acid reported for *R. bracarensis* (Albuquerque et al., 2014) was identified as 12-methyl hexadece-11-noic acid based on its mass spectrum, a hydrogenation experiment (which increased the relative abundance of 12-methyl hexadecanoic acid), and DMDS derivatization followed by GC–MS analysis. It represents the only unsaturated fatty acid identified. Other moderately abundant fatty acids (≥2%) included *n*-$C_{18:0}$, *ai*-$C_{17:0}$ and *n*-$C_{15:0}$, and an unidentified trimethyl pentadecanoic acid (Table 2). Remarkably, the 1-MGEs represented 36–46 % of the total lipids of *R. radiotolerans*, *R. xylanophilus* and *R. bracarensis* (Table 2). These lipids have largely been overlooked in other studies, except for Carreto et al. (Carreto et al., 1996), who spotted their presence in *R. xylanophilus* and *R. radiotolerans* as "a pair of isomeric l-heptadecyl-2,3-di-O-trimethylsilyl glycerols". The MGEs detected comprised a complex mixture composed of 1-MGEs with a variety of ether-bound alkyl moieties (Table 2), which varied in distribution between the three strains. In *R. bracarensis* the *ai*-$C_{19:0}$ dominated, whereas in *R. radiotolerans* *ai*-$C_{17:0}$ and *n*-$C_{18:0}$ represented the most abundant alkyl moieties. *R. xylanophilus* revealed the most complex distribution with *ai*-$C_{17:0}$ being the most abundant component.

*R. calidifluminis* and *R. naiadicus* exhibited similar core lipid distributions (Table 2), which were clearly distinct from those of *R. radiotolerans*, *R. xylanophilus* and *R. bracarensis* as previously noted (Albuquerque et al., 2014). In this study the presence of one major unidentified fatty acid was noted in both strains, in addition to *i*-$C_{17:0}$ and *i*-$C_{18:0}$ fatty acids. The fatty acid profiles of our cultures of *R. calidifluminis* and *R. naiadicus* (Table 2) differ from those reported earlier (Albuquerque et al., 2014). The *i*-$C_{17:0}$ fatty acid is indeed a prominent fatty acid but the *i*-$C_{18:0}$ fatty acid is present in lower abundance. However, the most abundant fatty acid (25–28 % of the total lipids; Table 2) was identified as an ω-cyclohexyl $C_{19:0}$ fatty acid by mass spectral characterization (Fig. 1a). The mass spectrum of its methyl derivative reveals a molecular ion at *m/z* 310, suggesting it to be a $C_{19:1}$ fatty acid but hydrogenation did not affect it. The mass spectrum also showed a clear *m/z* 83 ion, which is an indication for the presence of a cyclohexyl moiety and is virtually identical to that of a synthesized standard (Marseglia et al., 2013). This ω-cyclohexyl $C_{19:0}$ fatty acid was not reported in the earlier study (Albuquerque et al., 2014) but probably reflects the unknown fatty acid with an equivalent chain length (ECL) of 19.10, which occurred only in *R. naiadicus* in relatively low abundance (ca. 1 %). A later eluting fatty acid was identified as 10-methyl ω-cyclohexyl $C_{19:0}$ fatty acid. The mass spectrum of its methyl derivative (Fig. 1b) showed a molecular ion at *m/z* 324 and a clear *m/z* 83 fragment ion, indicative of a $C_{20}$ fatty acid with a ω-cyclohexyl moiety. In good agreement, it was not affected by hydrogenation. Its relative retention time indicates that it is not a homologue of the ω-cyclohexyl $C_{19:0}$ fatty acid but that the alkyl chain contains a methyl group. The enhanced fragment ion at *m/z* 199 suggests it to be at position 10 (Fig. 1b). This is probably

**Table 1**
*Rubrobacter* strains used in this study

| Species | Origin | Optimal growth temperature (°C) | Specific traits | Reference |
|---|---|---|---|---|
| *R. radiotolerans* (DSM 5868 $^{T}$) | Radioactive hot spring (Misasa, Japan) | 45 | Radiotolerant, moderately thermophilic, slightly halotolerant | (Suzuki et al., 1988) |
| *R. bracarensis* VF70612_S1$^{T}$ (DSM 24908 $^{T}$) | Biodeteriorated interior walls of Vilar de Frades Church (Braga, Portugal) | 28-37 | Mesophilic, halotolerant | (Jurado et al., 2012) |
| *R. xylanophilus* PRD-1 $^{T}$ (DSM 9941 $^{T}$) | Thermally polluted runoff from a carpet factory (Wilton, UK) | 60 | Radiotolerant, thermophilic, slightly halotolerant | (Ferreira et al., 1999; Carreto et al., 1996) |
| *R. calidifluminis* RG-1 $^{T}$ (DSM 106799 $^{T}$) | Fumaroles at Ribeira Grande (São Miguel, Azores) | 60 | Thermophilic, highly desiccation resistant | (Albuquerque et al., 2014) |
| *R. naiadicus* RG-3 $^{T}$ (DSM 106800 $^{T}$) | Fumaroles at Ribeira Grande (São Miguel, Azores) | 60 | Thermophilic, slightly halotolerant, highly desiccation resistant | (Albuquerque et al., 2014) |

**Table 2**
Core lipid abundance (in % of total) of the five investigated *Rubrobacter* species. Relative abundances > 10 % are in bold font.

| Total number of carbon atoms of acyl or alkyl chains | Core lipid | *R. radiotolerans* | *R. xylanophilus* | *R. bracarensis* | *R. calidifluminis* | *R. naiadicus* |
|---|---|---|---|---|---|---|
| *Fatty acids* | | | | | | |
| 15 | *ai*-$C_{15:0}$ | 2.9 | – | – | – | – |
| 16 | *i*-$C_{16:0}$ | 0.6 | – | – | 0.8 | 0.3 |
| | *n*-$C_{16:0}$ | 1.8 | 0.9 | 0.7 | 0.6 | 0.4 |
| 17 | *i*-$C_{16:0}$ 10-methyl | – | – | – | 0.8 | 0.3 |
| | *n*-$C_{16:1}\Delta 11$ 12-methyl | – | – | 5.1 | – | – |
| | *n*-$C_{16:0}$ 12-methyl | **35.3** | 7.7 | **52.9** | – | – |
| | *i*-$C_{17:0}$ | – | – | – | **13.4** | **14.5** |
| | *ai*-$C_{17:0}$ | 2.1 | – | – | 1.8 | 1.5 |
| 18 | *n*-$C_{15:0}$ trimethyl | 4.3 | 2.0 | 2.5 | – | – |
| | *i*-$C_{17:0}$ 10-methyl | – | – | – | 3.4 | 7.9 |
| | *ai*-$C_{17:0}$ 10-methyl | – | – | – | 1.8 | 1.2 |
| | *n*-$C_{17:0}$ 12-methyl | – | 0.6 | – | – | – |
| | *i*-$C_{18:0}$ | – | – | – | 7.7 | 3.8 |
| | ω- cyclohexyl $C_{17:0}$ 8-methyl | – | – | – | 0.4 | 0.4 |
| | *n*-$C_{18:0}$ | 2.1 | 9.5 | – | 0.9 | 1.2 |
| 19 | *i*-$C_{18:0}$ 10/12-methyl | – | – | – | 1.4 | 0.8 |
| | *n*-$C_{18:0}$ 12-methyl | – | 1.9 | – | – | – |
| | *n*-$C_{18:0}$ 14-methyl | 5.4 | **36.7** | 2.9 | – | – |
| | *i*-$C_{19:0}$ | – | – | – | 1.1 | 0.8 |
| | *ai*-$C_{19:0}$ | – | – | – | 0.5 | 1.0 |
| | ω- cyclohexyl $C_{19:0}$ | – | – | – | **27.5** | **24.6** |
| 20 | $C_{17:0}$ trimethyl | – | 1.4 | – | – | – |
| | *ai*-$C_{19:0}$ 12-methyl | – | – | – | 3.8 | 5.0 |
| | ω- cyclohexyl $C_{19:0}$ 10-methyl | – | – | – | **13.4** | 9.0 |
| *1-MGEs* | | | | | | |
| 16 | *n*-$C_{16:0}$ | 8.6 | 1.7 | 4.7 | – | – |
| 17 | *i*-$C_{17:0}$ | 1.6 | 6.6 | 6.3 | 0.4 | 0.4 |
| | *ai*-$C_{17:0}$ | **17.0** | **10.8** | – | – | – |
| 18 | *n*-$C_{15:0}$ trimethyl | – | 1.4 | – | – | – |
| | *n*-$C_{17:0}$ 12-methyl | – | 0.6 | 1.0 | – | – |
| | *n*-$C_{18:0}$ | **13.7** | 5.8 | 2.2 | **14.2** | **21.5** |
| 19 | *n*-$C_{19:0}$ | – | 1.4 | – | 2.4 | 2.0 |
| | *i*-$C_{19:0}$ | – | 2.0 | 4.4 | – | – |
| | *ai*-$C_{19:0}$ | 4.6 | 7.5 | **16.4** | – | – |
| 20 | *n*-$C_{17:0}$ trimethyl | – | 1.6 | 1.0 | – | – |

the major (20–30 %) unknown fatty acid in *R. calidifluminis* and *R. naiadicus* with an ECL of 19.89 reported in an earlier study (Albuquerque et al., 2014).

1-MGEs were also detected in *R. calidifluminis* and *R. naiadicus* but were less abundant than in the other three species (17–24 %). Their distribution was also different since they were strongly dominated by the 1-MGE with an *n*-$C_{18:0}$ alkyl chain (Table 2).

*Intact polar lipids*

IPLs with 10 different head groups (see Fig. 2) were detected with UHPLC-HRMS$^n$ in the five *Rubrobacter* species investigated. They were semi-quantified based on the relative intensity of the $[M^+]$, $[M + H^+]$, or $[M + NH_4^+]$ ions (see Table 3). This allows comparison between the species but does not correspond directly to the absolute abundance since mass spectral response factors for different IPLs may vary. Based on this analysis, three head group IPL types were detected in all five species: phosphoglycerol (PG), sulfoquinovosyl (SQ) and phosphohexose (PHex). These IPL had a similar relative intensity in all five species but the relative intensity in *R. calidifluminis* and *R. naiadicus* (25–37 %) was higher than in the other three species (Fig. 3).

The IPL types, phosphocholine (PC), its structurally related counterpart, dimethyl phosphoethanolamine (DMPE), and an unknown IPL were only detected in *R. radiotolerans*, *R. xylanophilus* and *R. bracarensis*, with PC-IPLs with the highest abundance (ca. 40 %; Fig. 3). All members of the series of unknown IPLs gave rise to a $MS^2$ spectrum with a dominant diagnostic fragment ion at mass *m/z* 186.053, assigned as a $C_4H_{13}NO_5P$ ion, based on its accurate mass (Fig. 4). This elemental formula is comparable to the phosphothreonine headgroup ($C_4H_{11}NO_6P$, *m/z* 200.032), but lacking an oxygen atom and containing two more hydrogen atoms. We, therefore, tentatively assigned this headgroup as phosphothreoninol (PT; Fig. 2), the reduced form of phosphothreonine. Two other headgroup types were

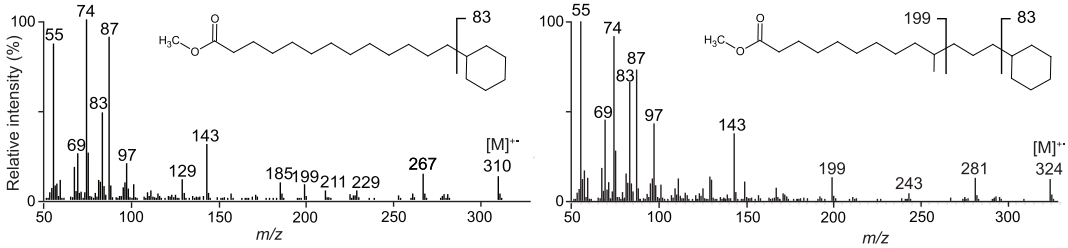


**Fig. 1.** Mass spectra of the methyl esters of the two novel ω-cyclohexyl fatty acids detected in *R. calidifluminis* RG-1 $^T$ and *R. naiadicus* RG-3 $^T$: (A) 13-cyclohexyl tridecanoic acid methyl ester and, (B) 10-methyl-13-cyclohexyl tridecanoic acid methyl ester.

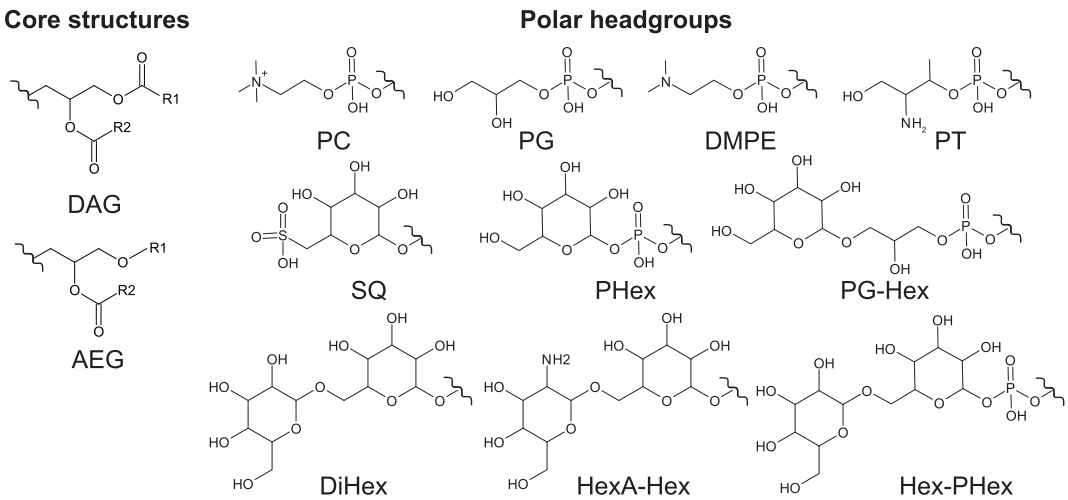


**Fig. 2.** Core structures and polar head groups and of the identified IPLs of the of five *Rubrobacter* species. Abbreviations: DAG = diacylglycerol, AEG = acyl/ether glycerol, PC = phosphocholine, PG = phosphoglycerol, DMPE = dimethyl phosphoethanolamine, PT = phosphothreoninol, SQ = sulfoquinovosyl, PHex = phosphohexose, PG-Hex = phosphoglycerol-hexose, DiHex = dihexose, HexA-Hex = hexosamine-hexose, Hex-PHex = hexose-phosphohexose.

only detected in *R. radiotolerans* in low abundance (ca. 3 %; Fig. 3), a dihexose (DiHex; possibly a digalactosyl) and a phosphoglycerol-hexose (PG-Hex).

Two series of IPLs of which the structure remains enigmatic were present only in *R. calidifluminis* and *R. naiadicus* but occurred in low abundance (Fig. 3). The first series comprised two lipids, which exhibited $[M + H]^+$ ions at *m/z* 1162.871 and 1176.886 (Table 2). These both exhibited a neutral loss in $MS^2$ of 341.135 Da, corresponding to an elemental composition of $C_{12}H_{23}NO_{10}$, assigned as a hexosamine-hexose (HexA-Hex) moiety. Indeed, for both components the $MS^2$ spectrum contained a fragment at *m/z* 162.076, equivalent to $C_6H_{12}NO_{10}$, as was seen previously for the same headgroup in the lipidome of the moderately acidophilic sulfur-reducing bacteria *'Acididesulfobacillus acetoxydans'* INE (Sánchez-Andrea et al., 2022). While the headgroup was identifiable, the core components were not. For the lipid with an $[M + H]^+$ at *m/z* 1162.871, upon loss of the hexosamine-hexose headgroup, a fragment ion was produced at *m/z* 821.734, equivalent to $C_{55}H_{97}O_4$. Assuming that the headgroup is attached to the apolar chains of the lipid by a glycerol moiety, this leaves 52 non-glycerol carbon atoms in the core component, along with two non-glycerol oxygen atoms. Similarly, on loss of the hexosamine-hexose headgroup from the lipid with an $[M + H]^+$ at *m/z* 1176.886 a fragment ion was produced at *m/z* 835.752, equivalent to $C_{56}H_{99}O_4$, which would, by the same reasoning as above, constitute a core with 53 non-glycerol carbon atoms and again two non-glycerol oxygen atoms. The second series of unidentified IPLs comprised four lipids with $[M + H]^+$ ions at *m/z* 1217.806, *m/z* 1231.821, *m/z* 1243.821 and *m/z* 1257.837. They all exhibited a neutral loss in $MS^2$ of 422.083 Da, assigned as $C_{12}H_{23}O_{10}P$, assigned as a hexose-phosphohexose (Hex-PHex) moiety. As per the HexA-Hex IPLs, this series contain an unidentified, large core-component, comprising presumably 50 – 53 non-glycerol carbon atoms.

Strikingly, for all these strains, all their IPLs had an acyl/ether glycerol core (termed AEGs (Sturt et al., 2004), except for the DiHex IPLs, which had a diacylglycerol (DAG) core, and, perhaps, the HexA-Hex and Hex-PHex IPLs, which have an unknown core. This means that > 90 % of all IPLs for all five species had an AEG core (Table 3). This is in good agreement with the high relative abundance of the 1-MGEs after acid hydrolysis of the Bligh-Dyer extracts (Table 2). Since 2-MGEs were not detected, it means that almost all IPLs (independent of the head group) possess an ether bound alkyl group at the *sn*-1 position.

When the alkyl/acyl distribution of the various IPL classes are considered, it is apparent that IPLs with one degree of unsaturation/number of rings (double bond equivalent) are mostly represented in the PG, SQ and PHex classes, but only in *R. calidifluminis* and *R. naiadicus* (Table 3). This is evidently the consequence of the fact that only these two species produce ω-cyclohexyl fatty acids (Table 2). The PC IPLs also contain some monounsaturated or -cyclic core lipids but only in *R. bracarensis*, which is the only one of the three PC IPL-containing species containing a monounsaturated fatty acid (i.e., 12-methyl hexadec-11-enoic acid). So, these PC IPLs contain this FA esterified at the *sn*-2 position with an *sn*-1 O-alkyl glycerol moiety. Individual AEG IPLs can be built up by varying both the nature of the ether-bound alkyl moiety and the esterified fatty acid, which leads to complex mixtures of IPLs. The LC-$HRMS^n$ analysis does not allow to reveal the number of carbon atoms contained in these individual moieties. Therefore, Table 3 denotes the total of non-glycerol carbon atoms. Nevertheless, in the case of in *R. calidifluminis* and *R. naiadicus*, where *n*-octadecyl forms the dominant ether-bound alkyl moiety (Table 2), it can be noted that the distribution of the individual AEG IPLs is in general a good reflection of their fatty acid distribution.

The intact polar lipids (IPLs) of *Rubrobacter* spp. have been studied in the past using two-dimensional TLC (e.g. (Carreto et al., 1996; Albuquerque et al., 2014; Chen et al., 2020). Generally, these analyses lead to somewhat unspecific results. Using two-dimensional TLC Albuquerque et al. (Albuquerque et al., 2014) reported for the five species examined here the presence of PG, a glycolipid, various phosphoglycolipids, various phospholipid, two aminolipids, and diphosphatidylglycerol (DPG). The spot pattern of *R. calidifluminis* and *R. naiadicus* was highly similar and less complex than that of the other three strains. However, the five spots recognized in the analysis of the IPLs of *R. calidifluminis* and *R. naiadicus* were all also recognized in the other three species, which is seemingly in contrast with our UHPLC-$HRMS^n$ results (Fig. 3) since both species do produce structurally distinct IPLs (i.e., Hex-AHex and Hex-PHex). Another substantial difference is that DPG was not detected by UHPLC-$HRMS^n$ in any of the species. However, the most important difference is that the results reported from these two-dimensional TLC analyses were always interpreted to indicate the presence of the common diacyl IPLs, whereas we show here that the major fraction (i.e., > 90 %) of the IPLs possess an AEG core structure. Hence, we conclude that for a state-of-the-art chemotaxonomic characterization of microbial cultures mass spectral analysis of the IPLs is a must.

**Table 3**
Composition and distribution of identified IPLs in the five *Rubrobacter* species. The summed relative abundance of IPLs with the same head group are provided in bold typeface.

| Polar headgroup | Glycerol core composition[a] | Measured Mass[b] | AEC[c] | Δ mmu[d] | Relative abundance (%)[e] | | | | |
|---|---|---|---|---|---|---|---|---|---|
| | | | | | *R. radiotolerans* | *R. xylanophilus* | *R. bracarensis* | *R. calidifluminis* | *R. naiadicus* |
| PC | AEG C33:0 | 734.6060 | $C_{41}H_{85}NO_7P$ | 0.2 | 8.8 | 1.1 | 0.8 | - | - |
| | AEG C34:0 | 748.6220 | $C_{42}H_{87}NO_7P$ | 0.5 | 10.5 | 6.6 | 13.5 | - | - |
| | AEG C34:1 | 746.6064 | $C_{42}H_{85}NO_7P$ | 0.5 | - | - | 4.6 | - | - |
| | AEG C35:0 | 762.6369 | $C_{43}H_{89}NO_7P$ | 0.3 | 9.5 | 5.8 | 2.2 | - | - |
| | AEG C35:1 | 760.6221 | $C_{43}H_{87}NO_7P$ | 0.7 | - | - | 1.0 | - | - |
| | AEG C36:0 | 776.6533 | $C_{44}H_{87}NO_7P$ | 0.1 | 5.7 | 12.1 | 8.9 | - | - |
| | AEG C36:1 | 774.6373 | $C_{44}H_{89}NO_7P$ | 0.2 | - | - | 4.9 | - | - |
| | AEG C37:0 | 790.6689 | $C_{45}H_{93}NO_7P$ | 0.5 | 3.0 | 6.6 | 2.4 | - | - |
| | AEG C37:1 | 788.6520 | $C_{45}H_{91}NO_7P$ | 0.7 | - | - | 0.3 | - | - |
| | AEG C38:0 | 804.6850 | $C_{46}H_{95}NO_7P$ | 0.5 | 1.4 | 8.2 | 1.0 | - | - |
| | AEG C39:0 | 818.7002 | $C_{47}H_{97}NO_7P$ | 0.5 | 0.3 | 3.2 | 0.1 | - | - |
| | **Total** | | | | **39.2** | **43.6** | **39.7** | **0** | **0** |
| PG | AEG C33:0 | 723.5529 | $C_{39}H_{80}O_9P$ | 0.6 | 1.3 | 0.4 | 0.3 | 0.4 | 0.3 |
| | AEG C34:0 | 737.5689 | $C_{40}H_{82}O_9P$ | 0.2 | 2.0 | 2.0 | 3.5 | 1.6 | 1.5 |
| | AEG C35:0 | 751.5846 | $C_{41}H_{84}O_9P$ | 0.1 | 2.1 | 1.9 | 1.0 | 2.4 | 3.6 |
| | AEG C36:0 | 765.6003 | $C_{42}H_{86}O_9P$ | 0.1 | 1.7 | 3.7 | 3.3 | 2.5 | 3.2 |
| | AEG C36:1 | 763.5846 | $C_{42}H_{84}O_9P$ | 0.1 | - | - | - | 4.4 | 3.0 |
| | AEG C37:0 | 779.6156 | $C_{43}H_{88}O_9P$ | 0.5 | 0.9 | 2.4 | 1.2 | 4.8 | 4.9 |
| | AEG C37:1 | 777.6001 | $C_{43}H_{86}O_9P$ | 0.3 | - | - | - | 3.1 | 3.2 |
| | AEG C38:0 | 793.6309 | $C_{44}H_{90}O_9P$ | 0.8 | 0.5 | 2.7 | 0.6 | 3.9 | 4.0 |
| | AEG C38:1 | 791.6161 | $C_{44}H_{88}O_9P$ | 0.1 | - | - | - | 2.2 | 2.3 |
| | AEG C39:0 | 807.6467 | $C_{45}H_{92}O_9P$ | 0.7 | 0.1 | 1.1 | 0.1 | 2.8 | 2.6 |
| | AEG C39:1 | 805.6314 | $C_{45}H_{90}O_9P$ | 0.3 | - | - | - | - | - |
| | AEG C40:0 | 821.6624 | $C_{46}H_{94}O_9P$ | 0.6 | 0.0 | 0.4 | 0.0 | - | - |
| | **Total** | | | | **8.6** | **14.6** | **10.0** | **28.1** | **28.6** |
| DMPE | AEG C33:0 | 720.5902 | $C_{40}H_{83}NO_7P$ | 0.1 | 2.9 | 0.2 | 0.3 | - | - |
| | AEG C34:0 | 734.6065 | $C_{41}H_{85}NO_7P$ | 0.7 | 3.8 | 1.4 | 5.2 | - | - |
| | AEG C35:0 | 748.6220 | $C_{42}H_{87}NO_7P$ | 0.5 | 3.5 | 1.6 | 1.4 | - | - |
| | AEG C36:0 | 762.6378 | $C_{43}H_{89}NO_7P$ | 0.7 | 2.3 | 3.8 | 4.8 | - | - |
| | AEG C37:0 | 776.6532 | $C_{44}H_{91}NO_7P$ | 0.5 | 0.8 | 2.0 | 0.7 | - | - |
| | AEG C38:0 | 790.6694 | $C_{45}H_{93}NO_7P$ | 1.0 | 0.4 | 1.9 | 0.3 | - | - |
| | **Total** | | | | **13.7** | **10.9** | **12.7** | **0** | **0** |
| PT | AEG C33:0 | 736.5855 | $C_{40}H_{83}NO_8P$ | 0.0 | 1.7 | 0.0 | 0.6 | - | - |
| | AEG C34:0 | 750.6008 | $C_{41}H_{85}NO_8P$ | 0.0 | 3.5 | 0.2 | 9.7 | - | - |
| | AEG C35:0 | 764.6172 | $C_{42}H_{87}NO_8P$ | 0.1 | 3.1 | 0.2 | 2.1 | - | - |
| | AEG C36:0 | 778.6321 | $C_{43}H_{89}NO_8P$ | 0.0 | 1.8 | 0.6 | 9.3 | - | - |
| | AEG C37:0 | 792.6460 | $C_{44}H_{91}NO_8P$ | 0.2 | 0.5 | 0.4 | 0.6 | - | - |
| | **Total** | | | | **10.6** | **1.4** | **22.3** | **0** | **0** |
| SQ | AEG C33:0 | 812.5915 | $C_{42}H_{86}NO_{11}S$ | 0.1 | 1.6 | 0.3 | 0.2 | 0.3 | 0.3 |
| | AEG C34:0 | 826.6065 | $C_{43}H_{88}NO_{11}S$ | 0.8 | 2.6 | 0.7 | 3.8 | 2.1 | 2.1 |
| | AEG C35:0 | 840.6224 | $C_{44}H_{90}NO_{11}S$ | 0.5 | 2.2 | 1.5 | 0.9 | 2.2 | 4.3 |
| | AEG C36:0 | 854.6382 | $C_{45}H_{92}NO_{11}S$ | 0.4 | 2.5 | 4.5 | 5.4 | 3.0 | 3.1 |
| | AEG C36:1 | 852.6219 | $C_{45}H_{90}NO_{11}S$ | 1.0 | - | - | - | 4.3 | 2.4 |
| | AEG C37:0 | 868.6534 | $C_{46}H_{94}NO_{11}S$ | 0.8 | 1.7 | 2.6 | 0.6 | 2.7 | 2.8 |
| | AEG C37:1 | 866.6377 | $C_{46}H_{92}NO_{11}S$ | 0.9 | - | - | - | 4.5 | 3.8 |
| | AEG C38:0 | 882.6692 | $C_{47}H_{96}NO_{11}S$ | 0.6 | 1.2 | 4.3 | 1.5 | - | 1.1 |
| | AEG C38:1 | 880.6535 | $C_{47}H_{94}NO_{11}S$ | 0.7 | - | - | - | 3.7 | 2.1 |
| | AEG C38:2 | 878.6388 | $C_{47}H_{92}NO_{11}S$ | 0.2 | - | - | - | 2.9 | 0.6 |
| | AEG C39:1 | 894.6720 | $C_{48}H_{96}NO_{11}S$ | 2.1 | - | - | - | 2.5 | 1.5 |
| | AEG C39:2 | 892.5636 | $C_{48}H_{94}NO_{11}S$ | 0.6 | - | - | - | 1.8 | 0.9 |
| | **Total** | | | | **11.8** | **13.9** | **12.4** | **30.0** | **25.0** |
| PHex | AEG C33:0 | 811.5689 | $C_{42}H_{84}O_{12}P$ | 0.6 | 1.5 | 0.6 | 0.1 | - | 0.5 |
| | AEG C34:0 | 825.5846 | $C_{43}H_{86}O_{12}P$ | 0.6 | 3.2 | 2.5 | 1.1 | 3.6 | 3.1 |
| | AEG C35:0 | 839.6005 | $C_{44}H_{88}O_{12}P$ | 0.3 | 2.7 | 2.4 | 0.4 | 4.1 | 5.5 |
| | AEG C36:0 | 853.6157 | $C_{45}H_{90}O_{12}P$ | 0.7 | 1.7 | 4.9 | 1.2 | 3.2 | 2.5 |
| | AEG C36:1 | 851.6003 | $C_{45}H_{88}O_{12}P$ | 0.5 | - | - | - | 3.2 | 3.9 |
| | AEG C37:0 | 867.6315 | $C_{46}H_{92}O_{12}P$ | 0.6 | 0.6 | 2.5 | 0.2 | 6.0 | 5.1 |
| | AEG C37:1 | 865.6163 | $C_{46}H_{90}O_{12}P$ | 0.1 | - | - | - | 2.9 | 3.6 |
| | AEG C38:0 | 881.6477 | $C_{47}H_{94}O_{12}P$ | 0.0 | 0.4 | 2.5 | - | 4.4 | 4.7 |
| | AEG C38:1 | 879.6315 | $C_{47}H_{92}O_{12}P$ | 0.6 | - | - | - | 0.0 | 1.8 |
| | AEG C39:1 | 893.6474 | $C_{48}H_{94}O_{12}P$ | 0.3 | - | - | - | 2.2 | 1.4 |
| | AEG C39:2 | 891.6321 | $C_{48}H_{92}O_{12}P$ | 0.0 | - | - | - | 2.8 | 3.3 |
| | AEG C40:1 | 907.6621 | $C_{49}H_{96}O_{12}P$ | 1.3 | - | - | - | 0.4 | 1.2 |
| | **Total** | | | | **10.1** | **15.4** | **3.0** | **32.8** | **36.6** |
| DiHex | DAG C31:0 | 896.6304 | $C_{46}H_{90}NO_{15}$ | 0.1 | 0.8 | - | - | - | - |
| | DAG C32:0 | 910.6454 | $C_{48}H_{92}NO_{15}$ | 0.8 | 1.7 | - | - | - | - |
| | DAG C33:0 | 924.6609 | $C_{49}H_{94}NO_{15}$ | 0.9 | 0.2 | - | - | - | - |
| | DAG C34:0 | 938.6765 | $C_{50}H_{96}NO_{15}$ | 1.0 | 0.6 | - | - | - | - |
| | **Total** | | | | **3.3** | **0** | **0** | **0** | **0** |

**Table 3** (*continued*)

| Polar headgroup | Glycerol core composition[a] | Measured Mass[b] | AEC[c] | Δ mmu[d] | Relative abundance (%)[e] | | | | |
|---|---|---|---|---|---|---|---|---|---|
| | | | | | *R. radiotolerans* | *R. xylanophilus* | *R. bracarensis* | *R. calidifluminis* | *R. naiadicus* |
| PG-Hex | AEG C33:0 | 885.6056 | $C_{45}H_{90}O_{14}P$ | 0.6 | 0.7 | - | - | - | - |
| | AEG C34:0 | 899.6211 | $C_{46}H_{92}O_{14}P$ | 0.9 | 1.0 | - | - | - | - |
| | AEG C35:0 | 913.6370 | $C_{47}H_{94}O_{14}P$ | 0.6 | 0.7 | - | - | - | - |
| | AEG C36:0 | 927.6530 | $C_{48}H_{96}O_{14}P$ | 0.2 | 0.3 | - | - | - | - |
| | **Total** | | | | **2.7** | **0** | **0** | **0** | **0** |
| HexA-Hex | C52 unknown | 1162.8713 | $C_{67}H_{120}O_{14}N$ | 0.1 | - | - | - | 0.3 | 1.9 |
| | C53 unknown | 1176.8862 | $C_{68}H_{122}O_{14}N$ | 0.0 | - | - | - | 0.1 | 1.1 |
| | **Total** | | | | **0** | **0** | **0** | **0.4** | **3.0** |
| Hex-PHex | C50 unknown | 1217.8058 | $C_{65}H_{118}O_{18}P$ | 0.1 | - | - | - | 0.5 | 0.5 |
| | C51 unknown | 1231.8213 | $C_{66}H_{120}O_{18}P$ | 0.1 | - | - | - | 0.4 | 0.7 |
| | C52 unknown | 1243.8208 | $C_{67}H_{120}O_{18}P$ | 0.0 | - | - | - | 5.6 | 3.5 |
| | C53 unknown | 1257.8370 | $C_{68}H_{122}O_{18}P$ | 0.1 | - | - | - | 2.1 | 2.0 |
| | **Total** | | | | **0** | **0** | **0** | **8.6** | **6.7** |

[a]Cx:y denotes the total of non-glycerol carbon atoms (x) and the number of unsaturation's or rings (y). In view of the near absence of unsaturated lipids after acid hydrolysis and the presence of cyclohexyl FAs (Table 2), IPLs with y = 1 mostly represent cyclohexyl fatty acids esterified at the sn-2 position of the glycerol moiety. [b]all masses represent an $[M + H]^+$ ion except PCs which are $[M]^+$ and the DiHexs and SQs which are $[M + NH_4]^+$. [c]assigned elemental composition. [d]the difference between the measured mass and AEC in milli mass units, [e]relative abundance based on the sum of all listed IPLs.

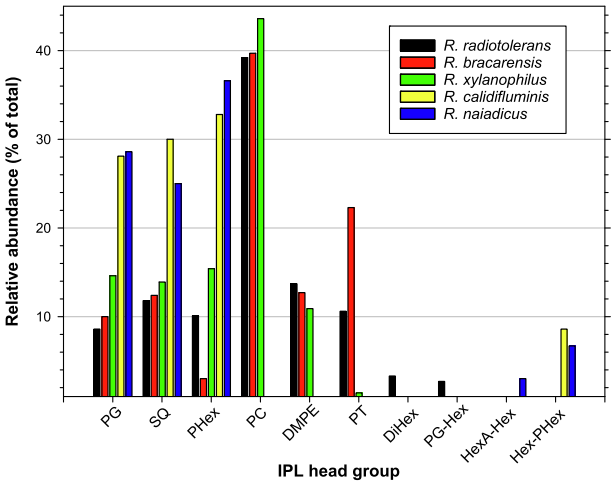


**Fig. 3.** Distribution of head groups of the identified IPLs of the five *Rubrobacter* species. For abbreviations of the polar head groups of the IPLs, see the caption of Fig. 2.

*Implications for phylogeny and biosynthesis of lipids*

The five investigated *Rubrobacter* species are phylogenetically related: their 16S rRNA gene sequences differ at maximum 11 % (Albuquerque et al., 2014) (see also Fig. 5a). Nevertheless, our lipid characterization showed substantial differences between *R. calidifluminis* and *R. naiadicus*, on the one hand, and *R. radiotolerans*, *R. xylanophilus* and *R. bracarensis*, on the other. Firstly, the IPL profile showed significant differences (Figs. 3 and 5b). Secondly, the fatty acid profiles contrasted substantially; the clearest difference being the abundance of ω-cyclohexyl fatty acids and absence of ω-4 methyl fatty acids in *R. calidifluminis* and *R. naiadicus*, while the opposite holds for the other three species (Fig. 5b). From a phylogenetic perspective, this does not make sense since the 16S rRNA gene sequence of *R. xylanophilus* is much more similar (1.6-1.7 %) to those of *R. calidifluminis* and *R. naiadicus* (Fig. 5a) than to those of *R. radiotolerans* and *R. bracarensis* (10.4-11.0 %) (Albuquerque et al., 2014). Also, the physiological adaptation to temperature, which may be thought to be a main driver for a change in membrane lipid composition, does not explain this since *R. calidifluminis, R. naiadicus*, *R. xylanophilus* are thermophiles, while *R. radiotolerans* and *R. bracarensis* are moderate thermophiles, growing at substantially lower temperatures (Table 1). Hence, this difference in fatty acid profile may be related to subtle difference in the genomic composition of these species.

Considering the dominance of the unusual ω-4 methyl fatty acids in most *Rubrobacter* species, and their absence in *R. calidifluminis* and *R. naiadicus*, it could be hypothesized that the latter species produce their specific ω-cyclohexyl fatty acids from an internal cyclization involving the ω-methyl group and the methyl at the ω-4 position of the alkyl chain of the fatty acid, which would lead to the formation of a six-membered ring. Such a reaction would require the unusual condensation of two un-activated methyl groups. However, such reactions have recently been shown to be occur with the help of radical SAM proteins: in the production glycerol dibiphytanyl glycerol tetraethers by condensation of the tails of the phytanyl moieties of archaeol (Zeng et al., 2022; Lloyd et al., 2022) and in the production of membrane-spanning lipids in bacteria by condensation of two ω methyl groups of iso fatty acids or two ω-1 methylene groups of *n*-alkyl fatty acids (Sahonero-Canavesi et al., 2022).

On the other hand, ω-cyclohexyl fatty acids are known to be produced by a variety of phylogenetically diverse thermo- and mesophilic bacteria: *e.g.*, *Alicyclobacillus* species (see (Ciuffreda et al., 2015) for an overview), *Curtobacterium pussilum* (Suzuki et al., 1981), and *Propionibacterium cyclohexanicum* (Kusano et al., 1997). Interestingly, Suzuki and Komagata (Suzuki and Komagata, 1983) studied the fatty acid profiles of 19 different strains of *Curtobacterium* spp. and only those belonging to *C. pussilum* produced ω-cyclohexyl fatty acids, a situation similar to the one described here for the *Rubrobacter* genus. Likewise, not all *Alicyclobacillus* species produce ω-cyclohexyl fatty acids, some produce ω-cycloheptyl fatty acids, while other species produce none (Ciuffreda et al., 2015). Already in 1976, Dreher et al. (Dreher et al., 1976) demonstrated that non ω-cyclohexyl fatty acid producing bacteria were able to produce them when fed with cyclohexane carboxylic acid CoA thioester (CHC-CoA). CHC-CoA has been shown to act as the starter unit for the production of ω-cyclohexyl fatty acids in *A. acidocaldarius* (Moore et al., 1993). The genomes of ω-cyclohexyl fatty acid-producing bacteria contain specific operons that encode proteins that are responsible for the biosynthesis of CHC-CoA, through a branch of the shikimic acid pathway. In various *Streptomyces* spp. the operon for the production of CHC-CoA has been well documented and is part of much larger operons that encode the biosynthesis of complex natural products such as ansantrienin and other mycotrienins, and asuka-

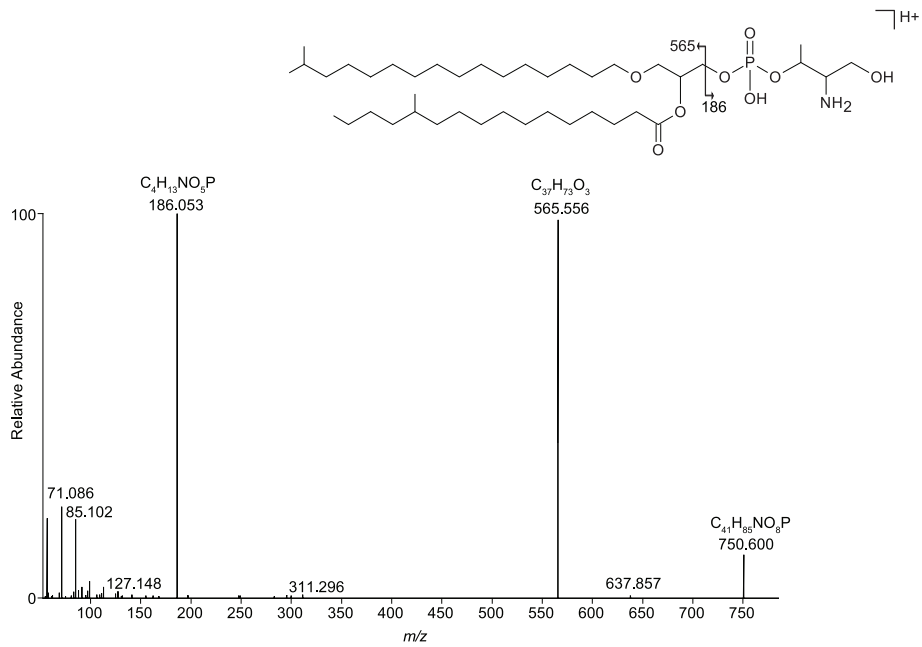


**Fig. 4.** An example of an $MS^2$ mass spectrum of an IPL containing the newly, tentatively identified, head group phosphothreoninol derived from analysis of IPLs by LC-HRMS. The accurate masses and corresponding elemental formulae of the $MH^+$ and some abundant fragments ions are indicated. This IPL contains an ether bound *iso* $C_{17}$ fatty acid at the *sn*-1 position and an ester bound 12-methyl hexadecanoic acid at the *sn*-2 position. 12-Methyl hexadecanoic acid belongs to the family of ω-4 methyl fatty acids.

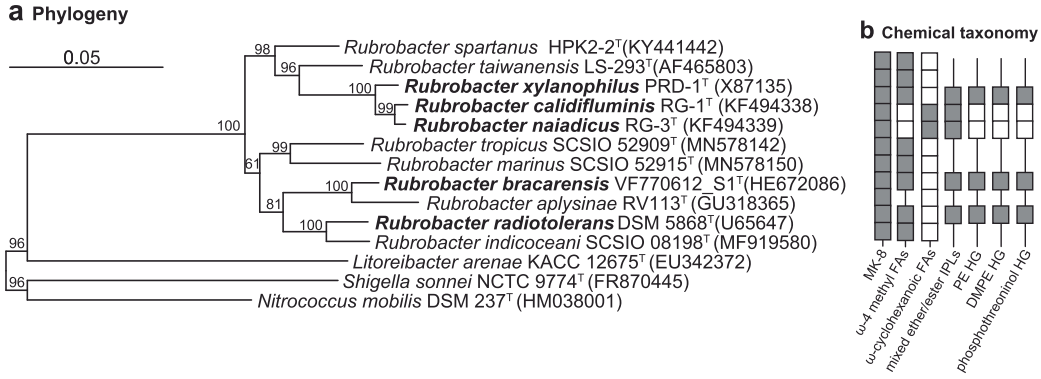


**Fig. 5.** Comparison of the phylogeny and chemical taxonomy for the *Rubrobacter* genus. (**a**) Phylogenetic neighbor-joining tree of the nearly complete 16S rRNA gene sequences of the eleven type strains of the *Rubrobacter* genus. GenBank accession numbers are provided in parentheses. Numbers at branch nodes refer to bootstrap values (1000 replicates). The bar indicates 5 substitutions per 100 sites. The five species studied for detailed lipid composition in this study are indicated in bold font. (**b**) Chemotaxonomic traits showing the presence (grey-filled square) or absence of specific lipids (white-filled square). The absence of a square indicates that no information is available. Data for menaquinones, provided for reference, was obtained from the literature (Yoshinaka et al., 1973; Suzuki et al., 1988; Ferreira et al., 1999; Carreto et al., 1996; Chen et al., 2004; Jurado et al., 2012; Albuquerque et al., 2014; Kämpfer et al., 2014; Norman et al., 2017; Chen et al., 2018; Chen et al., 2020). Data for fatty acids is from the literature (Albuquerque et al., 2014; Norman et al., 2017; Chen et al., 2018; Chen et al., 2020) and from this study (species in bold font). Note that no data is reported for *R. aplysinae* because the fatty acid distributions in Kämpfer et al. (Kämpfer et al., 2014) for *R. radiotolerans* does not correspond with data reported elsewhere (including this study), probably pointing to the difficulty to use the MIDI system for proper identification of mid-chain methyl branched fatty acids (see discussion in (Albuquerque et al., 2014). All data on IPLs and their head groups is from this study. Abbreviations: MK-8 = menaquinone-8, FAs = fatty acids, HG = head group.

mycins (e.g. (Cropp et al., 2000; Skyrud et al., 2020). It constitutes five genes (*ansJ-ansM,* of which the first two in some species are fused, and *chcA*), which together encode the proteins of a complex 9-step pathway in which shikimate is converted to CHC-CoA. Three genes (*chcA, ansJ* and *ansK*) of this operon have been extensively characterized (Skyrud et al., 2020; Wang et al., 1996). BLAST searches of the proteins encoded by the genomes of *R. calidifluminis* and *R. naiadicus* did reveal the presence of 4 of the 5 genes required for production of CHC-CoA and showed that they are organized in an operon (Table 4). The closest match within the *Streptomyces* group was with *S. humidus* (Table 4). This 4-gene operon, supposedly involved in the production of CHC-CoA, was not detected in the seven available NCBI reference genomes of *Rubrobacter* spp., which are all species not reported to produce ω-cyclohexyl fatty acids. Hence, the most plausible explanation for the biosynthesis of ω-cyclohexyl fatty acids in *R. calidifluminis* and *R. naiadicus* but not in any other *Rubrobacter* spp. is a recent acquisition of this operon, most likely by lateral gene transfer. However, the absence of the *ansM* gene remains a challenging question because Skyrud et al. (Skyrud et al., 2020) showed that all five genes were required in order to allow *E. coli* to produce CHC-CoA.

**Table 4**
Identification of the (partial) operon in *R. calidifluminis* and *R. naiadicus* responsible for encoding the proteins enabling the synthesis of CHC-CoA, the building block for the synthesis of W, by protein PSI-BLAST searches.

| *Streptomyces humidus* | | | | | *R. calidifluminis* | | | *R. naiadicus* | | |
|---|---|---|---|---|---|---|---|---|---|---|
| Encoding gene | Locus tag[a] | Protein[b] | Annotation[c] | Size[d] | Locus tag[a] | Similarity (%) | E-value | Locus tag[a] | Similarity (%) | E-value |
| *ansJ*[e] | IE239_RS33365 | WP_190153206.1 | 5-enolpyruvylshikimate-3-phosphate synthase | 1004 | PJB24_2521 | 48.8 | 1.9E-128 | PJB25_2794 | 48.6 | 3.0E-127 |
| *ansK*[e] | | | Coumarate-CoA ligase | | PJB24_2522 | 50.8 | 1.7E-165 | PJB25_2793 | 51.1 | 2.2E-167 |
| *ansL* | IE239_RS33360 | WP_190153205.1 | acyl-CoA dehydrogenase | 389 | PJB24_2523 | 56.4 | 9.2E-142 | PJB25_2792 | 56.3 | 1.4E-141 |
| *chcA* | IE239_RS33355 | WP_190153204.1 | 1-cyclohexenylcarbonyl-CoA reductase | 280 | PJB24_2524 | 57.2 | 1.6E-97 | PJB25_2791 | 57.2 | 2.1E-97 |
| *ansM* | IE239_RS33350 | WP_190153203.1 | 2,4-dienoyl-CoA reductase | 699 | - | - | - | - | - | - |

[a] locus tag from the NCBI database, [b] accession number from the NCBI database, [c] after Skyrud et al. (Skyrud et al., 2020); [d] number of amino acids of the protein, [e]*ansJ* and *ansK* genes are fused.

**Table 5**
Identification of a hypothetical operon in *Rubrobacter* spp. potentially involved in the synthesis of 1-O-alkyl glycerol phosphates, the building block for the abundant AEG-IPLs. The similarity of the proteins encoded by this operon are compared with proteins produced by *Myxococcus xanthus*, a known producer of 1-O-alkyl glycerol phosphates (Lorenzen et al., 2014).

| Species | Description[a] | Operon-constituting genes | | | |
|---|---|---|---|---|---|
| | | *plsY*[b] | *elbD* (partial)[c] | Dehydrogenase[d] | *elbC*[e] |
| *R. radiotolerans* | Locus tag | B9A07_RS11640 | B9A07_RS11635 | B9A07_RS11630 | B9A07_RS11625 |
| | Size | 203 | 752 | 401 | 526 |
| | Identity (%) | 42.3 | 28.2 | - | 48.4 |
| | E value | 1E-56 | 0 | - | 0 |
| *R. indicoceani* | Locus tag | DU509_RS04280 | DU509_RS04285 | DU509_RS04290 | DU509_RS04295 |
| | Size | 203 | 741 | 414 | 531 |
| | Identity (%) | 41.9 | 25.9 | - | 47.5 |
| | E value | 1E-58 | 0 | - | 0 |
| *R. tropicus* | Locus tag | GBA63_RS14075 | GBA63_RS14070 | GBA63_RS14060[e] | GBA63_RS14055 |
| | Size | 200 | 750 | 402 | 525 |
| | Identity (%) | 41.3 | 28.0 | - | 48.7 |
| | E value | 4E-58 | 0 | - | 0 |
| *R. xylanophilus* | Locus tag | RXYL_RS10605 | RXYL_RS16665 | RXYL_RS10595 | RXYL_RS10575 |
| | Size | 199 | 750 | 403 | 525 |
| | Identity (%) | 42.5 | 29.1 | - | 48.7 |
| | E value | 1E-56 | 0 | - | 0 |
| *R. taiwanensis* | Locus tag | E0L93_RS05930 | E0L93_RS05935 | E0L93_RS05940 | E0L93_RS05960 |
| | Size | 205 | 744 | 402 | 525 |
| | Identity (%) | 47.1 | 28.3 | - | 48.9 |
| | E value | 2E-61 | 0 | - | 0 |
| *R. calidifluminis* | Locus tag | PJB24_00179 | PJB24_00180 | PJB24_00181 | PJB24_00188 |
| | Size | 194 | 748 | 401 | 525 |
| | Identity (%) | 42.6 | 29.5 | - | 49.4 |
| | E value | 3E-41 | 2E-122 | - | 0 |
| *R. naiadicus* | Locus tag | PJB25_0919 | PJB25_0920 | PJB25_0921 | PJB25_0929 |
| | Size | 198 | 748 | 400 | 525 |
| | Identity (%) | 42.0 | 29.8 | - | 0 |
| | E value | 6E-41 | 7E-130 | - | 50.0 |

[a] locus tag from the NCBI database, size indicates the number of amino acids of the protein encode by the gene, identity (%) and E-value show values of matching parameters after two iterative PSI-BLAST searches
[b] PlsY of *M. xanthus* (WP_011551573.1, 192 amino acids) was used a query for the BLAST search
[c] ElbD of *M. xanthus* (WP_011551639.1, 1470 amino acids) was used a query for the BLAST search; only the first part of this multifunctional protein was encoded by this gene present in *Rubrobacter* spp.
[d] annotated to encode a zinc-binding dehydrogenase; not detected in the genome of *M. xanthus*
[e] together with GBA63_RS14065; these two locus tags encode the whole protein.

Another important finding of this study is that the membrane lipids of the five *Rubrobacter* spp. studied are predominantly (i.e., >90 %) composed of AEGs. This is unusual since it is considered to be textbook knowledge that bacterial membrane lipids are comprised of fatty acids esterified to a glycerol moiety forming DAGs. Nevertheless, ether lipids have been reported to occur in a few bacterial species, e.g., in some thermo- and mesophilic sulfate-reducing bacteria (Langworthy et al., 1983; Rütters et al., 2001; Grossi et al., 2015), in the thermophiles *Aquifex pyrophilus* and *Ammonifex degensii* (Huber et al., 1992; Huber et al., 1996), in a specific mesophilic clade of the Planctomycetes (Sinninghe Damsté et al., 2002; Sinninghe Damsté et al., 2005), in the myxobacterium *Myxococcus xanthus* DK1622 (Ring et al., 2006), in a few (hyper)thermophilic members of the bacterial phylum *Thermotogota* (Sinninghe Damsté et al., 2007; Sahonero-

Canavesi et al., 2022), and in aerobic and facultative anaerobic mesophilic bacteria of the Acidobacteriota subdivision 1 (Sinninghe Damsté et al., 2011); 4 (Sinninghe Damsté et al., 2014) , and, recently, 3 (Chen et al., 2022; Halamka et al., 2022). Two groups of enzymes responsible for bacterial ether lipid biosynthesis have been discovered. Jackson et al. (Jackson et al., 2020) identified in anaerobic bacteria a gene encoding a plasmalogen (an unsaturated ether) synthase (*plsA*). A modified form of *plsA* was subsequently detected in *Thermotoga maritima* and in other bacteria producing ether-derived lipids and was proposed to be involved in the direct conversion of bacterial ester bonds into ether bonds, generating saturated alkyl ethers (Sahonero-Canavesi et al., 2022). This was recently confirmed with the expression of this gene in *Escherichia coli* (Sahonero-Canavesi et al., 2022). In the aerobic myxobacteria, two independent pathways contributing to the biosynthesis of ether lipids have been identified; a gene coding for an alkylglycerone-phosphate synthase and the *elbB-elbE* gene cluster (Lorenzen et al., 2014). This putative operon has also been detected in subdivision 4 Acidobacteriota (i.e., *Blastocatellia*), which are the strictly aerobic and produce 1-MGEs in relatively high abundance (Sinninghe Damsté et al., 2018).

We searched for these genes in the genomes of *Rubrobacter* spp. and could not identify homologous of the *plsA* gene, which is in line with the fact that it only occurs in genomes of anaerobic bacteria (Sahonero-Canavesi et al., 2022). We also did not find the complete *elbB-elbE* gene cluster but detected a suspected operon that contains a part of the multifunctional *elbD* gene, a gene encoding a dehydrogenase, and *elbC* (Table 5). It is directly preceded by *plsY*, the gene encoding glycerol-3-phosphate acyltransferase, the protein catalyzing the first step of the biosynthesis of diacyl glycerol phosphate. This would suggest that this putative operon would encode proteins that are capable of directly reducing 1-acyl glycerol-3-phosphate formed by PlsY into 1-O-alkyl glycerol-3-phosphate, an appropriate starting biochemical to produce AEG IPLs that occur so abundantly in the *Rubrobacter* spp. The putative operon was detected, mostly in complete format, in the seven available NCBI reference genomes of *Rubrobacter* spp. and also in the here reported genomes of *R. calidifluminis* and *R. naiadicus* (Table 5). Future work will have to confirm our hypothesis that this putative operon is indeed involved in the formation of AEG IPLs.

## Conclusions

This study has identified the previously unknown fatty acids of *R. calidifluminis* and *R. naiadicus* as (methylated) ω-cyclohexyl fatty acids, not reported before to occur in *Rubrobacter* spp. These two species are also distinct from other known *Rubrobacter* spp. because they do not synthesize ω-4 methylated fatty acids, like all other isolated *Rubrobacter* spp. In addition, their IPL composition is dissimilar from those of three other studied *Rubrobacter* spp.; they do not produce PE-, DMPE-, and PT-IPLs but uniquely biosynthesize Hex-AHex and Hex-PHex-IPLs. A recent acquisition of an operon encoding proteins for the production of HCH-CoA, most likely by lateral gene transfer, is the most plausible explanation for the biosynthesis of ω-cyclohexyl fatty acids in *R. calidifluminis* and *R. naiadicus* but not in any other *Rubrobacter* spp.

All five studied *Rubrobacter* spp. are characterized by the dominance (>90 %) of AEG IPLs. This is uncommon because most bacteria produce DAGs as their core membrane lipids. All of the *Rubrobacter* spp. contain a putative operon (including *plsY*) in their genomes that may encode proteins enabling the direct production of 1-O-alkyl glycerol phosphate, the presumed primary building block for the AEG IPLs. The dominance of ether membrane lipids in *Rubrobacter* spp. serves as a nice illustration that the so-called 'lipid divide' between archaea and bacteria/eukaryotes is not as clear-cut as previously thought, in line with recent studies (Sahonero-Canavesi et al., 2022; Villanueva et al., 2017; Villanueva et al., 2021).

## CRediT authorship contribution statement

**Jaap S. Sinninghe Damsté:** Conceptualization, Formal analysis, Investigation, Writing – original draft, Writing – review & editing, Visualization, Supervision, Project administration, Funding acquisition. **W. Irene C. Rijpstra:** Investigation, Writing – review & editing. **Katharina J. Huber:** Investigation, Writing – review & editing. **Luciana Albuquerque:** Formal analysis, Investigation, Writing – review & editing, Funding acquisition. **Conceição Egas:** Formal analysis, Investigation, Writing – review & editing, Funding acquisition. **Nicole J. Bale:** Formal analysis, Investigation, Writing – original draft, Writing – review & editing, Visualization.

## Data availability

All data is available in the published manuscript or stored in public databases

## Declaration of Competing Interest

The authors declare that they have no known competing financial interests or personal relationships that could have appeared to influence the work reported in this paper.

## Acknowledgements

We thank Dr Peter Schumann (Leibniz Institute DSMZ, Germany) for initiating this project and the late Prof Milton S. da Costa (University of Coimbra, Portugal) for providing two strains for this study. We thank Carolin Pilke and Alicia Geppert (both from DSMZ) for biomass production, Dr Ellen C. Hopmans (NIOZ) for support in IPL identification, and Alejandro Abdala (NIOZ) for help with bioinformatic data processing. We acknowledge two anonymous referees for their comments.

## Funding information

This study was supported by the European Research Council (ERC) under the European Union's Horizon 2020 research and innovation program (grant agreement no. 694569-MICROLIPIDS to JSSD) and by the Soehngen Institute for Anaerobic Microbiology (SIAM) through a Dutch Gravitation Grant (grant no. 024.002.002 to JSSD). LA and CE were supported by FEDER funds through the Operational Program for Competitiveness and Internationalisation - COMPETE 2020 and Portuguese national funds by FCT - Foundation for Science and Technology under projects UIDB/04539/2020, UIDP/04539/2020, LA/P/0058/2020, and POCI-01-0145-FEDER-022184.

## References

Albuquerque, L., Johnson, M.M., Schumann, P., Rainey, F.A., da Costa, M.S., 2014. Description of two new thermophilic species of the genus *Rubrobacter*, *Rubrobacter calidifluminis* sp. nov. and *Rubrobacter naiadicus* sp. nov., and emended description of the genus *Rubrobacter* and the species *Rubrobacter bracarensis*. Syst. Appl. Microbiol. 37, 235–243.

Bale, N.J., Sorokin, D.Y., Hopmans, E.C., Koenen, M., Rijpstra, W.I.C., Villanueva, L., Wienk, H., Sinninghe Damsté, J.S., 2019. New insights into the polar lipid composition of extremely halo(alkali)philic euryarchaea from hypersaline lakes. Front. Microbiol. 10, 00377.

Bale, N.J., Ding, S., Hopmans, E.C., Arts, M.G., Villanueva, L., Boschman, C., Haas, A.F., Schouten, S., Sinninghe Damste, J.S., 2021. Lipidomics of environmental microbial communities. I: visualization of component distributions using untargeted analysis of high-resolution mass spectrometry data. Front. Microbiol. 12, 659302.

Bankevich, A., Nurk, S., Antipov, D., Gurevich, A.A., Dvorkin, M., Kulikov, A.S., Lesin, V. M., Nikolenko, S.I., Pham, S., Prjibelski, A.D., Pyshkin, A.V., Sirotkin, A.V., Vhahhi, N., Tesler, G., Alekseyev, M.A., Pevzner, P.A., 2012. SPAdes: a new genome assembly algorithm and its applications to single-cell sequencing. J. Comput. Biol. 19, 455–477.

Bolger, A.M., Lohse, M., Usadel, B., 2014. Trimmomatic: a flexible trimmer for Illumina sequence data. Bioinformatics 30, 2114–2120.

Carreto, L., Moore, E., Nobre, M.F., Wait, R., Riley, P.W., Sharp, R.J., da Costa, M.S., 1996. *Rubrobacter xylanophilus* sp. nov., a new thermophilic species isolated from a thermally polluted effluent. Int. J. Syst. Evol. Microbiol. 46, 460–465.

Chen, R.W., Wang, K.X., Wang, F.Z., He, Y.Q., Long, L.J., Tian, X.P., 2018. *Rubrobacter indicoceani* sp. nov., a new marine actinobacterium isolated from Indian Ocean sediment. Intern. J. Syst. Evol. Microbiol. 68, 3487–3493.

Chen, R.W., Li, C., He, Y.Q., Cui, L.Q., Long, L.J., Tian, X.P., 2020. *Rubrobacter tropicus* sp. nov. and *Rubrobacter marinus* sp. nov., isolated from deep-sea sediment of the South China Sea. Intern. J. Syst. Evol. Microbiol. 70, 5576–5585.

Chen, R.W., He, Y.Q., Cui, L.Q., Li, C., Shi, S.B., Long, L.J., Tian, X.P., 2021. Diversity and distribution of uncultured and cultured *Gaiellales* and *Rubrobacterales* in South China Sea sediments. Front. Microbiol. 12, 657072.

Chen, M.Y., Wu, S.H., Lin, G.H., Lu, C.P., Lin, Y.T., Chang, W.C., Tsay, S.S., 2004. *Rubrobacter taiwanensis* sp. nov., a novel thermophilic, radiation-resistant species isolated from hot springs. Intern. J. Syst. Evol. Microbiol. 54, 1849–1855.

Chen, Y., Zheng, F., Yang, H., Yang, W., Wu, R., Liu, X., Liang, H., Chen, H., Pei, H., Zhang, C., Pancost, R.D., Zeng, Z., 2022. The production of diverse brGDGTs by an Acidobacterium providing a physiological basis for paleoclimate proxies. Geochim. Cosmochim. Acta 377, 155–165.

Ciuffreda, E., Bevilacqua, A., Sinigaglia, M., Corbo, M.R., 2015. *Alicyclobacillus* spp.: new insights on ecology and preserving food quality through new approaches. Microorganisms 3, 625–640.

Cropp, T.A., Wilson, D.J., Reynolds, K.A., 2000. Identification of a cyclohexylcarbonyl CoA biosynthetic gene cluster and application in the production of doramectin. Nature Biotechnol. 18, 980–983.

Dreher, R., Poralla, K., König, W.A., 1976. Synthesis of ω-alicyclic fatty acids from cyclic precursors in *Bacillus subtilis*. J. Bacteriol. 127, 1136–1140.

Ferreira, A.C., Nobre, M.F., Moore, E., Rainey, F.A., Battista, J.R., da Costa, M.S., 1999. Characterization and radiation resistance of new isolates of *Rubrobacter radiotolerans* and *Rubrobacter xylanophilus*. Extremophiles 3, 235–238.

Grossi, V., Mollex, D., Vinçon-Laugier, A., Hakil, F., Pacton, M., Cravo-Laureau, C., 2015. Mono- and dialkyl glycerol ether lipids in anaerobic bacteria: biosynthetic insights from the mesophilic sulfate reducer *Desulfatibacillum alkenivorans* PF2803T. Appl. Environm. Microbiol. 81, 3157–3168.

Halamka, T. A., Raberg, J. H., McFarlin, J. M., Younkin, A. D., Mulligan, C., Liu, X. L., Kopf, S. H. (2022) Production of diverse brGDGTs by Acidobacterium *Solibacter usitatus* in response to temperature, pH, and $O_2$ provides a culturing perspective on brGDGT proxies and biosynthesis. Geobiology, gbi.12525

Holmes, A.J., Bowyer, J., Holley, M.P., O'Donoghue, M., Montgomery, M., Gillings, M. R., 2000. Diverse, yet-to-be-cultured members of the *Rubrobacter* subdivision of the Actinobacteria are widespread in Australian arid soils. FEMS Microbiol. Ecol. 33, 111–120.

Huber, H., Rossnagel, P., Woese, C.R., Rachel, R., Langworthy, T.A., Stetter, K.O., 1996. Formation of ammonium from nitrate during chemolithoautotrophic growth of the extremely thermophilic bacterium *Ammonifex degensii* gen. nov. sp. nov. Syst. Appl. Microbiol. 19, 40–49.

Huber, R., Wilharm, T., Huber, D., Trincone, A., Burggraf, S., Konig, H., Reinhard, R., Rockinger, I., Fricke, H., Stetter, K.O., 1992. *Aquifex pyrophilus* gen. nov. sp. nov., represents a novel group of marine hyperthermophilic hydrogen-oxidizing bacteria. Syst. Appl. Microbiol. 15, 340–351.

Hyatt, D., Chen, G.L., Locascio, P.F., Land, M.L., Larimer, F.W., Hauser, L.J., 2010. Prodigal: prokaryotic gene recognition and translation initiation site identification. BMC Bioinformatics 11, 119.

Jackson, D.R., Cassilly, C.D., Plichta, D.R., Vlamakis, H., Liu, H., Melville, S.B., Xavier, J. R., Clardy, J., 2020. Plasmalogen biosynthesis by anaerobic bacteria: identification of a two-gene operon responsible for plasmalogen production in *Clostridium perfringens*. ACS Chem. Biol. 16, 6–13.

Jurado, V., Miller, A.Z., Alias-Villegas, C., Laiz, L., Saiz-Jimenez, C., 2012. *Rubrobacter bracarensis* sp. nov., a novel member of the genus *Rubrobacter* isolated from a biodeteriorated monument. Syst. Appl. Microbiol. 35, 306–309.

Kämpfer, P., Glaeser, S.P., Busse, H.J., Abdelmohsen, U.R., Hentschel, U., 2014. *Rubrobacter aplysinae* sp. nov., isolated from the marine sponge *Aplysina aerophoba*. Intern. J. Syst. Evol. Microbiol. 64, 705–709.

Kusano, K., Yamada, H., Niwa, M., Yamasato, K., 1997. *Propionibacterium cyclohexanicum* sp. nov., a new acid-tolerant ω-cyclohexyl fatty acid-containing propionibacterium isolated from spoiled orange juice. Intern. J. Syst. Evol. Microbiol. 47, 825–831.

Langworthy, T.A., Holzer, G., Zeikus, J.G., Tornabene, T.G., 1983. Iso- and anteiso-branched glycerol diethers of the thermophilic anaerobe *Thermodesulfotobacterium commune*. Syst. Appl. Microbiol. 4, 1–17.

Lloyd, C.T., Iwig, D.F., Wang, B., Cossu, M., Metcalf, W.W., Boal, A.K., Booker, S.J., 2022. Discovery, structure, mechanism of a tetraether lipid synthase. Nature 609, 197–203.

Lorenzen, W., Ahrendt, T., Bozhüyük, K.A., Bode, H.B., 2014. A multifunctional enzyme is involved in bacterial ether lipid biosynthesis. Nature Chem. Biol. 10, 425–427.

Marseglia, A., Caligiani, A., Comino, L., Righi, F., Quarantelli, A., Palla, G., 2013. Cyclopropyl and ω-cyclohexyl fatty acids as quality markers of cow milk and cheese. Food Chem. 140, 711–716.

Moore, B.S., Poralla, K., Floss, H.G., 1993. Biosynthesis of the cyclohexanecarboxylic acid starter unit of ω-cyclohexyl fatty acids in *Alicyclobacillus acidocaldarius*. J. Amer. Chem. Soc. 115, 5267–5274.

Nichols, P.D., Guckert, J.B., White, D.C., 1986. Determination of monosaturated fatty acid double-bond position and geometry for microbial monocultures and complex consortia by capillary GC-MS of their dimethyl disulphide adducts. J. Microbiol. Meth. 5, 49–55.

Nielsen, P., Fritze, D., Priest, F.G., 1995. Phenetic diversity of alkaliphilic *Bacillus* strains: proposal for nine new species. Microbiology 141, 1745–1761.

Norman, J.S., King, G.M., Friesen, M.L., 2017. *Rubrobacter spartanus* sp. nov., a moderately thermophilic oligotrophic bacterium isolated from volcanic soil. Intern. J. Syst. Evol. Microbiol. 67, 3597–3602.

Oren, A., Garrity, G.M., 2021. Valid publication of the names of forty-two phyla of prokaryotes. Intern. J. Syst. Evol. Microbiol. 71, 005056.

Parks, D.H., Imelfort, M., Skennerton, C.T., Hugenholtz, P., Tyson, G.W., 2015. CheckM: assessing the quality of microbial genomes recovered from isolates, single cells, and metagenomes. Genome Res. 25, 1043–1055.

Ring, M.W., Schwär, G., Thiel, V., Dickschat, J.S., Kroppenstedt, R.M., Schulz, S., Bode, H.B., 2006. Novel iso-branched ether lipids as specific markers of developmental sporulation in the myxobacterium *Myxococcus xanthus*. J. Biol. Chem. 281, 36691–36700.

Rütters, H., Sass, H., Cypionka, H., Rullkötter, J., 2001. Monoalkylether phospholipids in the sulfate-reducing bacteria *Desulfosarcina variabilis* and *Desulforhabdus amnigenus*. Arch. Microbiol. 176, 435–442.

Sahonero-Canavesi, D.X., Siliakus, M., Asbun, A.A., Koenen, M., von Meijenfeldt, F.B., Boeren, S., Bale, N.J., Engelman, J.C., Fiege, K., Strack van Schijndel, L., Sinninghe Damsté, J.S., Villanueva, L., 2022. Disentangling the lipid divide: Identification of key enzymes for the biosynthesis of unusual membrane-spanning and ether lipids in Bacteria. Science Adv. 8, eabq8652.

Sahonero-Canavesi, D., Villanueva, L., Bale, N.J., Bosviel, J., Koenen, M., Hopmans, E.C., Sinninghe Damsté, J.S., 2022. Changes in the distribution of membrane lipids during growth of *Thermotoga maritima* at different temperatures: Indications for the potential mechanism of biosynthesis of ether-bound diabolic acid (membrane-spanning) lipids. Appl. Environm. Microbiol. 88, e0176321.

Salam, N., Jiao, J.Y., Zhang, X.T., Li, W.J., 2020. Update on the classification of higher ranks in the phylum *Actinobacteria*. Intern. J. Syst. Evol. Microbiol. 70, 1331–1355.

Sánchez-Andrea, I., van der Graaf, C.M., Hornung, B., Bale, N.J., Jarzembowska, M., Sousa, D.Z., Rijstra, W.I.C., Sinninghe Damsté, J.S., Stams, A.J., 2022. Acetate degradation at low pH by the moderately acidophilic sulfate reducer *Acididesulfobacillus acetoxydans* gen. nov. sp. nov. Front. Microbiol. 13, 816605.

Seemann, T., 2014. Prokka: rapid prokaryotic genome annotation. Bioinformatics 30, 2068–2069.

Sinninghe Damsté, J.S., Strous, M., Rijpstra, W.I.C., Hopmans, E.C., Geenevasen, J.A., van Duin, A.C., van Niftrik, L.A., Jetten, M.S., 2002. Linearly concatenated cyclobutane lipids form a dense bacterial membrane. Nature 419, 708–712.

Sinninghe Damsté, J.S., Rijpstra, W.I.C., Geenevasen, J.A., Strous, M., Jetten, M.S., 2005. Structural identification of ladderane and other membrane lipids of planctomycetes capable of anaerobic ammonium oxidation (anammox). FEBS J. 272, 4270–4283.

Sinninghe Damsté, J.S., Rijpstra, W.I.C., Hopmans, E.C., Schouten, S., Balk, M., Stams, A. J., 2007. Structural characterization of diabolic acid-based tetraester, tetraether and mixed ether/ester, membrane-spanning lipids of bacteria from the order Thermotogales. Arch. Microbiol. 188, 629–641.

Sinninghe Damsté, J.S., Rijpstra, W.I.C., Hopmans, E.C., Weijers, J.W., Foesel, B.U., Overmann, J., Dedysh, S.N., 2011. 13,16-Dimethyl octacosanedioic acid (*iso*-diabolic acid), a common membrane-spanning lipid of Acidobacteria subdivisions 1 and 3. Appl. Environm. Microbiol. 77, 4147–4154.

Sinninghe Damsté, J.S., Rijpstra, W.I.C., Hopmans, E.C., Foesel, B.U., Wüst, P.K., Overmann, J., Tank, M., Bryant, D.A., Dunfield, P.F., Houghton, K., Stott, M.B., 2014. Ether- and ester-bound iso-diabolic acid and other lipids in members of Acidobacteria subdivision 4. Appl. Environm. Microbiol. 80, 5207–5218.

Sinninghe Damsté, J.S., Rijpstra, W.I.C., Foesel, B.U., Huber, K.J., Overmann, J., Nakagawa, S., Kim, J.J., Dunfield, P.F., Dedysh, S.N., Villanueva, L., 2018. An overview of the occurrence of ether- and ester-linked iso-diabolic acid membrane lipids in microbial cultures of the Acidobacteria: Implications for brGDGT paleoproxies for temperature and pH. Org. Geochem. 124, 63–76.

Skyrud, W., Flores, A.D.R., Zhang, W., 2020. Biosynthesis of cyclohexanecarboxyl-CoA highlights a promiscuous shikimoyl-CoA synthetase and a FAD-dependent dehydratase. ACS Catalysis 10, 3360–3364.

Sturt, H.F., Summons, R.E., Smith, K., Elvert, M., Hinrichs, K.U., 2004. Intact polar membrane lipids in prokaryotes and sediments deciphered by high-performance liquid chromatography/electrospray ionization multistage mass spectrometry—new biomarkers for biogeochemistry and microbial ecology. Rap. Comm. Mass Spectrom. 18, 617–628.

Suzuki, K.I., Komagata, K., 1983. Taxonomic significance of cellular fatty acid composition in some coryneform bacteria. Intern. J. Syst. Evol. Microbiol. 33, 188–200.

Suzuki, K.I., Saito, K., Kawaguchi, A., Okuda, S., Komagata, K., 1981. Occurrence of ω-cyclohexyl fatty acids in *Curtobacterium pusillum* strains. J. Gen. Appl. Microbiol. 27, 261–266.

Suzuki, K.I., Collins, M.D., Iijima, E., Komagata, K., 1988. Chemotaxonomic characterization of a radiotolerant bacterium, *Arthrobacter radiotolerans*: description of *Rubrobacter radiotolerans* gen. nov., comb. nov. FEMS Microbiol. Lett. 52, 33–40.

Villanueva, L., Schouten, S., Sinninghe Damsté, J.S., 2017. Phylogenomic analysis of lipid biosynthetic genes of Archaea shed light on the 'lipid divide'. Environm. Microbiol. 19, 54–69.

Villanueva, L., von Meijenfeldt, F.A., Westbye, A.B., Yadav, S., Hopmans, E.C., Dutilh, B. E., Sinninghe Damsté, J.S., 2021. Bridging the membrane lipid divide: Bacteria of the FCB group superphylum have the potential to synthesize archaeal ether lipids. ISME J. 15, 168–182.

Wang, P., Denoya, C.D., Morgenstern, M.R., Skinner, D.D., Wallace, K.K., DiGate, R., Patton, S., Banavali, N., Schuler, G., Speedie, M.K., Reynolds, K.A., 1996. Cloning and characterization of the gene encoding 1-cyclohexenylcarbonyl coenzyme A reductase from *Streptomyces collinus*. J. Bacteriol. 178, 6873–6881.

Yoshinaka, T., Yano, K., Yamaguchi, H., 1973. Isolation of highly radioresistant bacterium, *Arthrobacter radiotolerans* nov. sp. Agric. Biol. Chem. 37, 2269–2275.

Zeng, Z., Chen, H., Yang, H., Chen, Y., Yang, W., Feng, X., Pei, H., Welander, P.V., 2022. Identification of a protein responsible for the synthesis of archaeal membrane-spanning GDGT lipids. Nature Comm. 13, 1–9.